

# LINEAR, SECOND ORDER AND UNCONDITIONALLY ENERGY STABLE SCHEMES FOR THE VISCOUS CAHN-HILLIARD EQUATION WITH HYPERBOLIC RELAXATION

XIAOFENG YANG <sup>†</sup> AND JIA ZHAO <sup>‡</sup>

**ABSTRACT.** In this paper, we consider the numerical approximations for the fourth order viscous Cahn-Hilliard equation with the hyperbolic relaxation. The main challenge in solving such a diffusive system numerically is how to develop high order temporal discretization for the hyperbolic and nonlinear terms that allows large time step while preserving the unconditional energy stability, i.e., the energy dissipative structure at the time-discrete level. We resolve this issue by developing two second order time marching schemes using the recently developed “Invariant Energy Quadratization” approach where all nonlinear terms are treated semi-explicitly. In each time step, one only needs to solve a linear system that is symmetric positive definite. We rigorously prove all proposed schemes are unconditionally energy stable, which is further verified by time step refinement test numerically. Moreover, a number of 2D and 3D numerical simulations are presented to demonstrate the stability, accuracy and efficiency of the proposed schemes.

## 1. INTRODUCTION

The viscous Cahn-Hilliard (VCH) system and/or its perturbed version with a hyperbolic relaxation (HR) effect, had been well-studied recently, where the topics are mainly focused on the well-posedness, sharp interface limit or global attractor, etc., see [2, 3, 6, 9–11, 14, 15, 17–19, 23–30, 33, 35, 40, 43–45, 54] and the references therein. Formally, the governing equation of the VCH-HR system is slightly different from the most classical Cahn-Hilliard (CH) equation, that is proposed by Cahn and Hillard in [5], by incorporating a strong damping term (or called “viscosity”) and a hyperbolic relaxation term (or called “inertia”). The viscosity term is firstly proposed by Novick-Cohen in [43] to introduce an additional regularity and some parabolic smoothing effects. Its system can be viewed as a singular limit of the phase field equations for phase transitions (cf. [18]). The hyperbolic relaxation term was proposed by Galenko et. al. in [23–28, 35], in order to describe strongly non-equilibrium decomposition generated by rapid solidification under supercooling into the spinodal region occurring in certain materials (e.g., glasses). Since the VCH-HR system combines the hyperbolic relaxation and the viscosity together, it is mathematically more complicated and tractable than the CH or VCH system (cf. [33, 45, 67]).

Before developing efficient numerical schemes to solve the VCH-HR system, we notice that its reduced version, the classical CH equation is now widely applied to model the interfacial dynamics in various scientific fields (cf. [5, 7, 16, 34, 36, 39, 41, 55] and the references therein). The CH equation and its analogous counterpart, the Allen-Cahn equation, are both categorized as representative equations of *phase field* type models. From the numerical point of view, although all unknown variables in phase field models are continuous and smooth, the induced systems are still very stiff

---

*Key words and phrases.* Phase-field, Linear, Cahn-Hilliard, Energy Stability, Second order, Invariant Energy Quadratization.

<sup>†</sup>Corresponding author, Department of Mathematics, University of South Carolina, Columbia, SC 29208; Email: xfyang@math.sc.edu.

<sup>‡</sup>Department of Mathematics, University of North Carolina at Chapel Hill, 27599; Email: zhaojia@email.unc.edu.

where the stiffness is induced by the order parameter representing the thickness of the interface. Therefore, when solving such stiff systems, it is desirable to establish efficient numerical schemes that can verify the so called “energy stable” property at the discrete level irrespectively of the coarseness of the discretization. In what follows, those algorithms will be called *unconditionally energy stable* or *thermodynamically consistent*. Schemes with this property is specially preferred since it is not only critical for the numerical scheme to capture the correct long time dynamics of the system, but also provides sufficient flexibility for dealing with the stiffness issue. In spite of this, it is necessary to point out a basic fact that larger time step will definitely induce larger computational errors. In other words, the schemes with *unconditional* energy stability can allow *unconditionally* large time step only for the sake of the stability concern. In practice, the controllable accuracy is one of the most important factors to measure whether a scheme is reliable or not. Therefore, if one attempts to use the time step as large as possible while maintaining desirable accuracy, the only possible solution is to develop more accurate schemes, e.g., the second order schemes with unconditionally energy stability, that is the main focus of this paper.

It is remarkable that, unlike the enormous numerical studies on the classical CH system, almost all research related to the VCH or VCH-HR system had been focused on the theoretical PDE analysis with very few numerical analysis or algorithm design. More precisely, to the best of the authors’ knowledge, no schemes have been claimed to posses the following three properties, namely, easy-to-implement, unconditionally energy stability and second order accuracy for the VCH-HR model. This is because two additional numerical difficulties, the discretization of the viscous effect as well as the hyperbolic inertia, emerge except the regular stiffness issue induced by the nonlinear double well potential. At the very least, even for the reduced version, the CH system, the algorithm design is still challenging. It can be seen clearly from the following fact that some severe stability conditions on the time step will occur if the nonlinear term is discretized in some normal ways like fully implicit or explicit type approaches. Such a time step constraint can cause very high the computational cost in practice [4, 21, 49]. Many efforts (primarily for CH system) had been done in order to remove this constraint and two commonly used techniques were developed, namely, the nonlinear convex splitting approach [20, 31, 54, 56], and the linear stabilized approach [8, 37, 38, 42, 46–53, 58, 59, 61, 63, 65, 66]. The convex splitting approach is unconditionally energy stable, but it produces the nonlinear scheme, thus the implementation is complicated and the computational cost might be high. The linear stabilized approach is linear so it is efficient and very easy to implement. But, its stability requests a special property (generalized maximum principle) satisfied by the classical PDE solution and the numerical solution, that is very hard to prove in general. Moreover, it is difficult to extend to second-order while preserving the unconditional energy stability (cf. [49]).

Therefore, in order to develop some more efficient and accurate time marching schemes for solving the VCH-HR equation, we use the *Invariant Energy Quadraticization* (IEQ) approach, which has been successfully applied to solve various phase field type models, see the authors’ recent work in [57, 60, 62, 64]. Its idea, that is very simple but quite different from those traditional methods like implicit, explicit, nonlinear splitting, or other various tricky Taylor expansions to discretize the nonlinear potentials, is to make the free energy *quadratic*. To be more specific, the free energy potential is transformed into the quadratic form forcefully via the change of variables. Then, upon a simple reformulation, all nonlinear terms are treated by the semi-explicit way, which in turn yields a linear system. We develop two second order schemes, in which, one is based on the Crank-Nicolson, and the other is based on the Adam-Bashforth (BDF2). These schemes are not only *easy-to-implement* (linear system), but also *unconditionally energy stable* (with a discrete energy dissipation law). Moreover, we show that the linear operator of all schemes are *symmetric positive*

*definite*, so that one can solve it using the well-developed fast matrix solvers efficiently (CG or other Krylov subspace methods). Through various 2D and 3D numerical simulations, we demonstrate stability and accuracy of the proposed schemes.

The rest of the paper is organized as follows. In Section 2, we present the whole system and show the energy law in the continuous level. In Section 3, we develop the numerical schemes and prove their unconditional stabilities. In Section 4, we present various 2D and 3D numerical experiments to validate the accuracy and efficiency of the proposed numerical schemes. Finally, some concluding remarks are presented in Section 5.

## 2. MODEL EQUATIONS

Now we give a brief description for the model equations. We consider a binary alloy in a bounded domain  $\Omega \in \mathbb{R}^d, d = 2, 3$  with  $\partial\Omega$  Lipschitz continuous, and define  $\phi(\mathbf{x}, t)$  as relative concentration of one material component,  $\mathbf{J}$  the diffusion flux, then the balance law for concentration gives

$$(2.1) \quad \phi_t + \nabla \cdot \mathbf{J} = 0.$$

In order to describe the evolution for  $\phi$ , one need to introduce a constitutive assumption on  $\mathbf{J}$ , i.e.,

$$(2.2) \quad \alpha \mathbf{J}_t + \mathbf{J} = -\nabla \left( \frac{\delta E}{\delta \phi} + \beta \phi_t \right).$$

Here  $E(\phi)$  is the total free energy that takes the form as

$$(2.3) \quad E(\phi) = \int_{\Omega} \left( \frac{\epsilon^2}{2} |\nabla \phi|^2 + F(\phi) \right) d\mathbf{x},$$

where  $\alpha \geq 0$  is the relaxation parameter,  $\beta \geq 0$  is the viscosity parameter, and  $\epsilon$  is the positive constant that measures the interfacial width.

For the choice of nonlinear potential  $F(\phi)$ , we can choose either (i) double well (Ginzburg-Landau) potential where

$$(2.4) \quad F(\phi) = \phi^2(\phi - 1)^2;$$

or (ii) Flory-Huggins potential (cf. [45]) where

$$(2.5) \quad F(\phi) = (1 - \phi) \ln(1 - \phi) + \phi \ln \phi + \theta \phi(1 - \phi), \theta > 0.$$

By combining (2.1) and (2.2), the governing PDE reads as follows,

$$(2.6) \quad \alpha \phi_{tt} + \phi_t = \lambda \Delta \mu,$$

$$(2.7) \quad \mu = -\epsilon^2 \Delta \phi + f(\phi) + \beta \phi_t,$$

where  $f(\phi) = F'(\phi)$ , i.e.,  $f(\phi) = 2\phi(\phi - 1)(2\phi - 1)$  for double well potential and  $f(\phi) = \ln(\frac{\phi}{1-\phi}) + \theta(1 - 2\phi)$  for Flory-Huggins potential. The boundary conditions can be

$$(2.8) \quad (i) \text{ all variables are periodic; or } (ii) \partial_{\mathbf{n}} \phi|_{\partial\Omega} = \partial_{\mathbf{n}} \mu|_{\partial\Omega} = 0,$$

where  $\mathbf{n}$  is the unit outward normal on  $\partial\Omega$ .

When  $\alpha = \beta = 0$ , the system degenerates to the standard CH system that conserves the local mass density. When  $\alpha \neq 0$ , the volume conservation will only hold provided  $\int_{\Omega} \phi_t(0, \mathbf{x}) d\mathbf{x} = 0$ . To see this, by taking the  $L^2$  inner product of (2.6) with 1, one can obtain directly

$$(2.9) \quad \alpha \frac{d}{dt} \int_{\Omega} \phi_t(t, \mathbf{x}) d\mathbf{x} + \int_{\Omega} \phi_t(t, \mathbf{x}) d\mathbf{x} = 0.$$

This actually is an ODE system for time, and its solution is

$$(2.10) \quad \int_{\Omega} \phi_t(t, \mathbf{x}) d\mathbf{x} = \exp\left(\frac{-t}{\alpha}\right) \int_{\Omega} \phi_t(0, \mathbf{x}) d\mathbf{x}.$$

Therefore, by setting  $\int_{\Omega} \phi_t(0, \mathbf{x}) d\mathbf{x} = 0$ , we obtain

$$(2.11) \quad \int_{\Omega} \phi_t(t, \mathbf{x}) d\mathbf{x} = \int_{\Omega} \phi_{tt}(t, \mathbf{x}) d\mathbf{x} = 0.$$

Here and after, for any functions  $g_1(\mathbf{x}), g_2(\mathbf{x}) \in L^2(\Omega)$ , we denote the inner product and  $L^2$  norm as

$$(2.12) \quad (g_1, g_2) = \int_{\Omega} g_1(\mathbf{x}) g_2(\mathbf{x}) d\mathbf{x}, \quad \|g_1\| = \int_{\Omega} |g_1(\mathbf{x})|^2 d\mathbf{x}.$$

We define the inverse Laplace operator  $u \in L^2(\Omega)$  with  $\int_{\Omega} u d\mathbf{x} = 0 \mapsto v := \Delta^{-1}u$  ( $v \in H^1(\Omega)$ ) by

$$(2.13) \quad \begin{cases} \Delta v = u, & \int_{\Omega} u d\mathbf{x} = 0, \\ \text{with the boundary conditions either (i) } v \text{ is periodic, or (ii) } \partial_{\mathbf{n}} v|_{\partial\Omega} = 0. \end{cases}$$

**Lemma 2.1.** *The model system (2.6)-(2.7) satisfies an energy dissipation law as,*

$$(2.14) \quad \frac{d}{dt} \int_{\Omega} \left( \frac{\epsilon^2}{2} |\nabla \phi|^2 + F(\phi) + \frac{\alpha}{2} |\nabla \Delta^{-1} \phi_t|^2 \right) d\mathbf{x} = -\|\nabla \Delta^{-1} \phi_t\|^2 - \beta \|\phi_t\|^2 \leq 0.$$

*Proof.* We introduce a new variable  $\psi = \phi_t$ . Since  $\int_{\Omega} \psi d\mathbf{x} = \int_{\Omega} \psi_t d\mathbf{x} = 0$ , using the operator  $\Delta^{-1}$ , we rewrite the system (2.6)-(2.7) as follows,

$$(2.15) \quad \alpha \Delta^{-1} \psi_t + \Delta^{-1} \psi = -\epsilon^2 \Delta \phi + f(\phi) + \beta \phi_t.$$

By taking the  $L^2$  inner product of (2.15) with  $\phi_t$ , we have

$$(2.16) \quad \alpha(\Delta^{-1} \psi_t, \psi) + (\Delta^{-1} \psi, \psi) - \beta \|\phi_t\|^2 = \frac{d}{dt} \int_{\Omega} \left( \frac{\epsilon^2}{2} |\nabla \phi|^2 + F(\phi) \right) d\mathbf{x}.$$

Since  $\int_{\Omega} \psi d\mathbf{x} = 0$ , we can find another auxillary variable  $p$  such that  $p = \Delta^{-1} \psi$ , i.e.,

$$(2.17) \quad \Delta p = \psi, \quad \int_{\Omega} \psi d\mathbf{x} = 0,$$

with the boundary condition specified in (2.13). By taking the  $L^2$  inner product of (2.17) with  $p$ , that is

$$(2.18) \quad (p, \psi) = -\|\nabla p\|^2 = (\Delta^{-1} \psi, \psi).$$

We differentiate (2.17) with time  $t$  to obtain

$$(2.19) \quad \Delta p_t = \psi_t.$$

By taking the  $L^2$  inner product of (2.19) with  $p$ , we obtain  $(\psi_t, p) = (\Delta p_t, p) = -\frac{1}{2} d_t \|\nabla p\|^2$ . Hence, we derive

$$(2.20) \quad \alpha(\Delta^{-1} \psi_t, \psi) = \alpha(\psi_t, \Delta^{-1} \psi) = \alpha(\psi_t, p) = -\frac{\alpha}{2} d_t \|\nabla p\|^2.$$

By combining (2.16)-(2.18)-(2.20), we obtain

$$(2.21) \quad \frac{d}{dt} \int_{\Omega} \left( \frac{\epsilon^2}{2} |\nabla \phi|^2 + F(\phi) + \frac{\alpha}{2} |\nabla p|^2 \right) d\mathbf{x} = -\|\nabla p\|^2 - \beta \|\phi_t\|^2 \leq 0.$$

This will ensure the modified energy of the VCH-HR system (2.6)-(2.7) nonincreasing in time.  $\square$

## 3. NUMERICAL SCHEMES

We now construct two semi-discrete time marching numerical schemes for solving the model system (2.6)-(2.7)-(2.8) and prove their energy stabilities based on the *Invariant Energy Quadratization* (IEQ) approach. The key point of the IEQ method is to make the nonlinear potential *quadratic* via the change of auxiliary variables. It is feasible since we notice that the nonlinear potential  $F(\phi)$  is always bounded from below, in either the double well form (for the Ginzberg-Landau potential) or logarithmic form (for the Flory-Huggins potential). Thus, in general, we could rewrite the free energy functional  $F(\phi)$  into the following equivalent form

$$(3.1) \quad F(\phi) = (F(\phi) + B) - B,$$

where  $B$  is some constant to ensure  $F(x) + B \geq 0, \forall x \in \mathbb{R}$ , and define an auxiliary function  $U$  as

$$(3.2) \quad U = \sqrt{F(\phi) + B}.$$

Thus the total energy of (2.3) turns to a new form

$$(3.3) \quad E(\phi, U) = \int_{\Omega} \left( \frac{\epsilon^2}{2} |\nabla \phi|^2 + U^2 - B \right) d\mathbf{x}.$$

Then we obtain an equivalent PDE system by taking the time derivative for the new variable  $U$ :

$$(3.4) \quad \alpha \psi_t + \psi = \Delta \mu,$$

$$(3.5) \quad \mu = -\epsilon^2 \Delta \phi + U H + \beta \phi_t,$$

$$(3.6) \quad U_t = \frac{1}{2} H \phi_t,$$

$$(3.7) \quad \psi = \phi_t,$$

where

$$(3.8) \quad H(\phi) = \frac{f(\phi)}{\sqrt{F(\phi) + B}}, \quad f(\phi) = F'(\phi).$$

The boundary conditions for the new system are still (2.8) since the equation (3.6) for the new variable  $U$  is simply an ODE with time. The initial conditions read as

$$(3.9) \quad \phi|_{(t=0)} = \phi_0, \psi|_{(t=0)} = 0,$$

$$(3.10) \quad U|_{(t=0)} = \sqrt{F(\phi_0) + B},$$

where we simply set the initial profile of  $\psi$  to be zero pointwise.

It is clear that the new transformed system (3.4)-(3.7) still retains a similar energy dissipative law. By applying the inverse Laplace operator  $\Delta^{-1}$  to (3.4), taking the  $L^2$  inner product of it with  $\phi_t$ , of (3.6) with  $-U$ , using (2.18) and (2.20), and summing them up, we can obtain the energy dissipation law of the new system (3.4)-(3.5) as

$$(3.11) \quad \frac{d}{dt} \int_{\Omega} \left( \frac{\epsilon^2}{2} |\nabla \phi|^2 + U^2 + \frac{\alpha}{2} |\nabla \Delta^{-1} \psi|^2 \right) d\mathbf{x} = -\|\nabla \Delta^{-1} \phi_t\|^2 - \beta \|\psi\|^2 \leq 0.$$

**Remark 3.1.** We emphasize that the new transformed system (3.4)-(3.7) is exactly equivalent to the original system (2.6)-(2.7), since (3.2) can be easily obtained by integrating (3.6) with respect to the time. For the time-continuous case, the potentials in the new free energy (3.3) are the same as the Lyapunov functional in the original free energy of (2.3), and the new energy law (3.11) for the transformed system is also the same as the energy law (2.14) for the original system as well. We will develop unconditionally energy stable numerical schemes for time stepping of the transformed

system (3.4)-(3.7), and the proposed schemes should formally follow the new energy dissipation law (3.11) in the discrete sense, instead of the energy law for the originated system (2.14).

**Remark 3.2.** If  $F(\phi) = \phi^2(\phi-1)^2$ , we let  $B = 0$ , thus  $H(\phi) = 2\phi-1$ . At this time, the IEQ method is exactly the same as the so-called Lagrange multiplier method developed in [32]. We remark that the Lagrange multiplier method in [32] only works for the fourth order polynomial potential ( $\phi^4$ ). This is because the term  $\phi^3$  (the first order derivative of  $\phi^4$ ) can be decomposed into a multiplication of two factors:  $\lambda(\phi)\phi$ , where  $\lambda(\phi) = \phi^2$ . In [32], this Lagrange multiplier term  $\lambda(\phi)$  is then defined as the new auxiliary variable  $U$ . However, for other type potentials, e.g., the F-H potential, if following the Lagrange method in [32], a new variable  $U$  will be defined as  $\lambda(\phi) = \frac{1}{\phi} \ln(\frac{\phi}{1-\phi})$ , which is unworkable for algorithms design.

**Remark 3.3.** If  $F(\phi) = (1-\phi)\log(1-\phi) + \phi\log\phi + \theta\phi(1-\phi)$ , following the work in [12], we regularize the logarithmic bulk potential by a  $C^2$  piecewise function. More precisely, for any  $0 < \sigma \ll 1$ , the regularized free energy is

$$(3.12) \quad \widehat{F}(\phi) = \begin{cases} \phi \ln \phi + \frac{(1-\phi)^2}{2\sigma} + (1-\phi) \ln \sigma - \frac{\sigma}{2} + \theta\phi(1-\phi), & \text{if } \phi \geq 1-\sigma, \\ \phi \ln \phi + (1-\phi) \ln(1-\phi) + \theta\phi(1-\phi), & \text{if } \sigma \leq \phi \leq 1-\sigma, \\ (1-\phi) \ln(1-\phi) + \frac{\phi^2}{2\sigma} + \phi \ln \sigma - \frac{\sigma}{2} + \theta\phi(1-\phi), & \text{if } \phi \leq \sigma. \end{cases}$$

For convenience, we consider the problem formulated with the substitute  $\widehat{F}(\phi)$ , but omit the  $\widehat{\phantom{x}}$  in the notation. Now the domain for the regularized functional  $F(\phi)$  is now  $(-\infty, \infty)$ . Hence, we do not need to worry about that any small fluctuation near the domain boundary  $(-1, 1)$  of the numerical solution can cause the overflow. In [12], the authors proved the error bound between the regularized PDE and the original PDE is controlled by  $\sigma$  up to a constant. For this case, we simply take  $B = 1$  that can ensure  $\widehat{F}(x) + B > 0, \forall x \in \mathbb{R}$ .

The time marching numerical schemes are developed to solve the new transformed system (3.4)-(3.7). The proof of the unconditional stability of the schemes follows the similar lines as in the derivation of the energy law (3.11). Let  $\delta t > 0$  denote the time step size and set  $t^n = n \delta t$  for  $0 \leq n \leq N$  with the ending time  $T = N \delta t$ .

**3.1. Crank-Nicolson Scheme.** We first develop a second order version that is based on the Crank-Nicolson, that reads as follows.

*Scheme 1.* Compute  $U^1$  and  $\phi^1$  by assuming  $U^{-1} = U^0$  and  $\phi^{-1} = \phi^0$  for the initial step. Having computed  $(\phi^n, U^n)$  and  $(\phi^{n-1}, U^{n-1})$ , with  $n \geq 1$ , we update  $\phi^{n+1}$  and  $U^{n+1}$  as follows:

$$(3.13) \quad \alpha \frac{\psi^{n+1} - \psi^n}{\delta t} + \frac{\psi^{n+1} + \psi^n}{2} = \Delta \mu^{n+1},$$

$$(3.14) \quad \mu^{n+1} = -\epsilon^2 \Delta \frac{\phi^{n+1} + \phi^n}{2} + \frac{U^{n+1} + U^n}{2} H^* + \beta \frac{\phi^{n+1} - \phi^n}{\delta t},$$

$$(3.15) \quad U^{n+1} - U^n = \frac{1}{2} H^* (\phi^{n+1} - \phi^n),$$

$$(3.16) \quad \frac{\psi^{n+1} + \psi^n}{2} = \frac{\phi^{n+1} - \phi^n}{\delta t},$$

where

$$(3.17) \quad H^* = \frac{f(\phi^*)}{\sqrt{F(\phi^*) + B}}, \quad \phi^* = \frac{3}{2}\phi^n - \frac{1}{2}\phi^{n-1}.$$

The boundary conditions are either

$$(3.18) \quad (i) \phi^{n+1}, \mu^{n+1} \text{ are periodic; or } (ii) \partial_{\mathbf{n}} \phi^{n+1}|_{\partial\Omega} = \nabla \mu^{n+1} \cdot \mathbf{n}|_{\partial\Omega} = 0.$$

Since the nonlinear coefficient  $H$  of the new variables  $U$  are treated explicitly, we can rewrite the equations (3.15) and (3.16) as follows:

$$(3.19) \quad \begin{cases} U^{n+1} = \frac{H^*}{2} \phi^{n+1} + g_1^n, \\ \psi^{n+1} = \frac{2}{\delta t} \phi^{n+1} + g_2^n, \end{cases}$$

where  $g_1^n = (U^n - \frac{H^*}{2} \phi^n)$ ,  $g_2^n = (-\frac{2}{\delta t} \phi^n - \psi^n)$ . Thus (3.13)-(3.14) can be rewritten as the following linear system

$$(3.20) \quad \hat{\alpha} \phi^{n+1} = \Delta \mu^{n+1} + g_3^n,$$

$$(3.21) \quad \mu^{n+1} = P_1(\phi^{n+1}) + g_4^n,$$

where

$$(3.22) \quad \begin{cases} \hat{\alpha} = (\frac{\alpha}{\delta t} + \frac{1}{2}) \frac{2}{\delta t}, \\ P_1(\phi^{n+1}) = -\frac{\epsilon^2}{2} \Delta \phi^{n+1} + \frac{1}{4} H^* H^* \phi^{n+1} + \frac{\beta}{\delta t} \phi^{n+1}, \\ g_3^n = -(\frac{\alpha}{\delta t} + \frac{1}{2}) g_2^n + (\frac{\alpha}{\delta t} - \frac{1}{2}) \psi^n, \\ g_4^n = -\frac{\epsilon^2}{2} \Delta \phi^n + \frac{1}{2} H^* (g_1^n + U^n) - \frac{\beta}{\delta t} \phi^n. \end{cases}$$

Therefore, we can solve  $\phi^{n+1}$  and  $\mu^{n+1}$  directly from (3.20) and (3.21). Once we obtain  $\phi^{n+1}$ , the  $\psi^{n+1}, U^{n+1}$  are automatically given in (3.19). Furthermore, for any  $\psi$  that enjoys the same boundary condition as  $\phi$  in (3.18), we have

$$(3.23) \quad (P_1(\phi), \psi) = \frac{\epsilon^2}{2} (\nabla \phi, \nabla \psi) + \frac{1}{4} (H^* \phi, H^* \psi) + \frac{\beta}{\delta t} (\phi, \psi).$$

Therefore, the linear operator  $P_1(\phi)$  is symmetric (self-adjoint). Moreover, for any  $\phi$  with  $\int_{\Omega} \phi d\mathbf{x} = 0$ , we have

$$(3.24) \quad (P_1(\phi), \phi) = \frac{\epsilon^2}{2} \|\nabla \phi\|^2 + \frac{1}{4} \|H^* \phi\|^2 + \frac{\beta}{\delta t} \|\phi\|^2 \geq 0,$$

where “=” is valid if and only if  $\phi \equiv 0$ .

We first show the well-posedness of the linear system (3.13)-(3.16) (or (3.20)-(3.21)) as follows.

**Theorem 3.1.** *The linear system (3.20)-(3.21) admits a unique solution in  $H^1(\Omega)$ , and the linear operator is symmetric positive definite.*

*Proof.* From (3.13), by taking the  $L^2$  inner product with 1 and notice  $\psi^0 = 0$ , we derive

$$(3.25) \quad (\frac{\alpha}{\delta t} + \frac{1}{2}) \int_{\Omega} \psi^{n+1} d\mathbf{x} = (\frac{\alpha}{\delta t} - \frac{1}{2}) \int_{\Omega} \psi^n d\mathbf{x} = 0.$$

From (3.16), we have

$$(3.26) \quad \int_{\Omega} \phi^{n+1} d\mathbf{x} = \int_{\Omega} \phi^n d\mathbf{x} = \dots = \int_{\Omega} \phi^0 d\mathbf{x}.$$

Let  $V_\phi = \frac{1}{|\Omega|} \int_\Omega \phi^0 d\mathbf{x}$ ,  $V_\mu = \frac{1}{|\Omega|} \int_\Omega \mu^{n+1} d\mathbf{x}$ , and we define

$$(3.27) \quad \widehat{\phi}^{n+1} = \phi^{n+1} - V_\phi, \quad \widehat{\mu}^{n+1} = \mu^{n+1} - V_\mu.$$

Thus, from (3.20)-(3.21),  $(\widehat{\phi}^{n+1}, \widehat{\mu}^{n+1})$  are the solutions for the following equations with unknowns  $(\phi, w)$ ,

$$(3.28) \quad \widehat{\alpha}\phi - \Delta w = f^n,$$

$$(3.29) \quad w + V_\mu - P_1(\phi) = g^n,$$

where  $f^n = g_3^n - \widehat{\alpha}V_\phi$ ,  $\int_\Omega f^n d\mathbf{x} = 0$ ,  $g^n = g_4^n + \frac{1}{4}H^*H^*\alpha_0 + \frac{\beta}{\delta t}\alpha_0$ ,  $\int_\Omega \phi d\mathbf{x} = 0$  and  $\int_\Omega w d\mathbf{x} = 0$ .

Applying  $-\Delta^{-1}$  to (3.28) and using (3.29), we obtain

$$(3.30) \quad -\widehat{\alpha}\Delta^{-1}\phi + P_1(\phi) - V_\mu = -\Delta^{-1}f^n - g^n.$$

Let us express the above linear system (3.30) as  $\mathbb{A}\phi = b$ ,

(i). For any  $\phi_1$  and  $\phi_2$  in  $H^1(\Omega)$  satisfy the boundary conditions (2.8) and  $\int_\Omega \phi_1 d\mathbf{x} = \int_\Omega \phi_2 d\mathbf{x} = 0$ , using integration by parts, we derive

$$(3.31) \quad \begin{aligned} (\mathbb{A}(\phi_1), \phi_2) &= -\widehat{\alpha}(\Delta^{-1}\phi_1, \phi_2) + (P_1(\phi_1), \phi_2) \\ &\leq C_1(\|\nabla\Delta^{-1}\phi_1\| \|\nabla\Delta^{-1}\phi_2\| + \|\nabla\phi_1\| \|\nabla\phi_2\| + \|\phi_1\| \|\phi_2\|) \\ &\leq C_2\|\phi_1\|_{H^1} \|\phi_2\|_{H^1}. \end{aligned}$$

Therefore, the bilinear form  $(\mathbb{A}(\phi_1), \phi_2)$  is bounded  $\forall \phi_1, \phi_2 \in H^1(\Omega)$ .

(ii). For any  $\phi \in H^1(\Omega)$ , it is easy to derive that,

$$(3.32) \quad (\mathbb{A}(\phi), \phi) = \widehat{\alpha}\|\nabla\Delta^{-1}\phi\|^2 + \frac{\epsilon^2}{2}\|\nabla\phi\|^2 + \frac{1}{4}\|H^*\phi\|^2 + \frac{\beta}{\delta t}\|\phi\|^2 \geq C_3\|\phi\|_{H^1}^2,$$

for  $\int_\Omega \phi d\mathbf{x} = 0$  from Poincare inequality. Thus the bilinear form  $(\mathbb{A}(\phi), \psi)$  is coercive.

Then from the Lax-Milgram theorem, we conclude the linear system (3.30) admits a unique solution in  $H^1(\Omega)$ .

For any  $\phi_1, \phi_2$  with  $\int_\Omega \phi_1 d\mathbf{x} = 0$  and  $\int_\Omega \phi_2 d\mathbf{x} = 0$ , we can easily derive

$$(3.33) \quad (\mathbb{A}\phi_1, \phi_2) = (\phi_1, \mathbb{A}\phi_2).$$

Thus  $\mathbb{A}$  is self-adjoint. Meanwhile, from (3.32), we derive  $(\mathbb{A}\phi, \phi) \geq 0$ , where “=” is valid if only if  $\phi = 0$ . This concludes the linear operator  $\mathbb{A}$  is positive definite.  $\square$

The energy stability of the scheme (3.13)-(3.16) (or (3.20)-(3.21)) is presented as follows.

**Theorem 3.2.** *The scheme (3.13)-(3.16) (or (3.20)-(3.21)) is unconditionally energy stable satisfying the following discrete energy dissipation law,*

$$(3.34) \quad \frac{1}{\delta t}(E_{cn2}^{n+1} - E_{cn2}^n) = -\left\|\frac{\nabla(p^{n+1} + p^n)}{2}\right\|^2 - \beta\left\|\frac{\phi^{n+1} - \phi^n}{\delta t}\right\|^2 \leq 0,$$

where

$$(3.35) \quad E_{cn2} = \frac{\epsilon^2}{2}\|\nabla\phi\|^2 + \|U\|^2 + \frac{\alpha}{2}\|\nabla p\|^2 - B|\Omega|.$$

*Proof.* First, we combine (3.13) and (3.14) together and apply the  $\Delta^{-1}$  to obtain

$$(3.36) \quad \begin{aligned} &\frac{\alpha}{\delta t}\Delta^{-1}(\psi^{n+1} - \psi^n) + \Delta^{-1}\frac{\psi^{n+1} + \psi^n}{2} \\ &= -\epsilon^2\Delta\frac{\phi^{n+1} + \phi^n}{2} + \frac{U^{n+1} + U^n}{2}H^* + \beta\frac{\phi^{n+1} - \phi^n}{\delta t}. \end{aligned}$$



Secondly, by taking the  $L^2$  inner product of (3.36) with  $\phi^{n+1} - \phi^n$ , we obtain

$$(3.37) \quad \begin{aligned} & \frac{\alpha}{\delta t}(\Delta^{-1}(\psi^{n+1} - \psi^n), \phi^{n+1} - \phi^n) + \frac{1}{2}(\Delta^{-1}(\psi^{n+1} + \psi^n), \phi^{n+1} - \phi^n) \\ &= \frac{\epsilon^2}{2}(\|\nabla \phi^{n+1}\|^2 - \|\phi^n\|^2) + \left(\frac{U^{n+1} + U^n}{2} H^*, \phi^{n+1} - \phi^n\right) + \frac{\beta}{\delta t} \|\phi^{n+1} - \phi^n\|^2. \end{aligned}$$

Thirdly, by taking the  $L^2$  inner product of (3.15) with  $-(U^{n+1} + U^n)$ , we obtain

$$(3.38) \quad -(\|U^{n+1}\|^2 - \|U^n\|^2) = -\left(\frac{1}{2} H^*(\phi^{n+1} - \phi^n), U^{n+1} + U^n\right).$$

Fourthly, define  $p^{n+1} = \Delta^{-1}\psi^{n+1}$ . By subtracting with the  $n$ -step, we obtain

$$(3.39) \quad \Delta(p^{n+1} - p^n) = \psi^{n+1} - \psi^n.$$

From (3.16) and (3.39), we derive

$$(3.40) \quad \begin{aligned} & \frac{\alpha}{\delta t}(\Delta^{-1}(\psi^{n+1} - \psi^n), \phi^{n+1} - \phi^n) = \frac{\alpha}{2}(p^{n+1} - p^n, \psi^{n+1} + \psi^n) \\ &= \frac{\alpha}{2}(p^{n+1} - p^n, \Delta(p^{n+1} + p^n)) \\ &= -\left(\frac{\alpha}{2} \|\nabla p^{n+1}\|^2 - \frac{\alpha}{2} \|\nabla p^n\|^2\right), \end{aligned}$$

and

$$(3.41) \quad \begin{aligned} & \frac{1}{2}(\Delta^{-1}(\psi^{n+1} + \psi^n), \phi^{n+1} - \phi^n) = \frac{\delta t}{4}(p^{n+1} + p^n, \psi^{n+1} + \psi^n) \\ &= \frac{\delta t}{4}(p^{n+1} + p^n, \Delta(p^{n+1} + p^n)) \\ &= -\frac{\delta t}{4} \|\nabla(p^{n+1} + p^n)\|^2. \end{aligned}$$

Finally, by combining (3.37), (3.38), (3.40) and (3.41), we obtain

$$(3.42) \quad \begin{aligned} & \frac{\epsilon^2}{2}(\|\nabla \phi^{n+1}\|^2 - \|\nabla \phi^n\|^2) + \|U^{n+1}\|^2 - \|U^n\|^2 + \frac{\alpha}{2}(\|\nabla p^{n+1}\|^2 - \|\nabla p^n\|^2) \\ &= -\frac{\delta t}{4} \|\nabla(p^{n+1} + p^n)\|^2 - \frac{\beta}{\delta t} \|\phi^{n+1} - \phi^n\|^2, \end{aligned}$$

that concludes the theorem.  $\square$

**Remark 3.4.** The proposed schemes follow the new energy dissipation law (3.11) formally instead of the energy law for the originated system (2.14). In the time-discrete case, the energy  $E(\phi^{n+1}, U^{n+1})$  (defined in (3.35)) can be rewritten as a first order approximation to the Lyapunov functionals in  $E(\phi^{n+1})$  (defined in (2.14)), that can be observed from the following facts, heuristically. Assuming the case for double well potential, from (3.15), we have

$$(3.43) \quad U^{n+1} - (\sqrt{F(\phi^{n+1}) + B}) = U^n - (\sqrt{F(\phi^n) + B}) + R_{n+1},$$

where  $R_{n+1} = O((\phi^{n+1} - \phi^n)(\phi^{n+1} - 2\phi^n + \phi^{n-1}))$ . Since  $R_k = O(\delta t^3)$  for  $0 \leq k \leq n+1$  and  $U^0 = (\sqrt{F(\phi^0) + B})$ , by mathematical induction we can easily get

$$(3.44) \quad U^{n+1} = \sqrt{F(\phi^{n+1}) + B} + O(\delta t^2).$$

**3.2. Adam-Bashforth Scheme.** We further develop another second order scheme based on the Adam-Bashforth backward differentiation formula (BDF2), as follows.

**Scheme 2.** Compute  $U^1$  and  $\phi^1$  by assuming  $U^{-1} = U^0$  and  $\phi^{-1} = \phi^0$  for the initial step. Having computed  $(\phi^n, U^n)$  and  $(\phi^{n-1}, U^{n-1})$ , with  $n \geq 1$ , we solve  $\phi^{n+1}, U^{n+1}$  as follows:

$$(3.45) \quad \alpha \frac{3\psi^{n+1} - 4\psi^n + \psi^{n-1}}{2\delta t} + \psi^{n+1} = \Delta\mu^{n+1},$$

$$(3.46) \quad \mu^{n+1} = -\epsilon^2 \Delta\phi^{n+1} + U^{n+1} H^\dagger + \beta \frac{3\phi^{n+1} - 4\phi^n + \phi^{n-1}}{2\delta t},$$

$$(3.47) \quad 3U^{n+1} - 4U^n + U^{n-1} = \frac{1}{2} H^\dagger (3\phi^{n+1} - 4\phi^n + \phi^{n-1}),$$

$$(3.48) \quad \psi^{n+1} = \frac{3\phi^{n+1} - 4\phi^n + \phi^{n-1}}{2\delta t}$$

where

$$(3.49) \quad H^\dagger = \frac{f(\phi^\dagger)}{\sqrt{F(\phi^\dagger) + B}}, \phi^\dagger = 2\phi^n - \phi^{n-1}.$$

The boundary conditions are

$$(3.50) \quad (i) \ \phi^{n+1}, \mu^{n+1} \text{ are periodic; or } (ii) \ \partial_{\mathbf{n}}\phi^{n+1}|_{\partial\Omega} = \nabla\mu^{n+1} \cdot \mathbf{n}|_{\partial\Omega} = 0.$$

Similar to the Crank-Nicolson scheme, we can rewrite the equations (3.47) and (3.48) as follows:

$$(3.51) \quad \begin{cases} U^{n+1} = \frac{H^\dagger}{2} \phi^{n+1} + h_1^n, \\ \psi^{n+1} = \frac{3}{2\delta t} \phi^{n+1} + h_2^n, \end{cases}$$

where  $h_1^n = (U^\pm - \frac{H^\dagger}{2} \phi^\pm)$ ,  $h_2^n = \frac{3}{2\delta t} \phi^\pm$  with  $S^\pm = \frac{4S^n - S^{n-1}}{3}$  for any variable  $S$ . Thus (3.45)-(3.46) can be rewritten as the following linear system

$$(3.52) \quad \tilde{\alpha} \phi^{n+1} = \Delta\mu^{n+1} + h_3^n,$$

$$(3.53) \quad \mu^{n+1} = P_2(\phi^{n+1}) + h_4^n,$$

where

$$(3.54) \quad \begin{cases} P_2(\phi^{n+1}) = -\epsilon^2 \Delta\phi^{n+1} + \frac{1}{2} H^\dagger H^\dagger \phi^{n+1} + \frac{3\beta}{2\delta t} \phi^{n+1}, \\ h_3^n = -(\frac{3\alpha}{2\delta t} + 1) h_2^n + \frac{3\alpha}{2\delta t} \psi^\pm, \\ h_4^n = \frac{1}{2} H^\dagger h_1^n - \frac{3\beta}{2\delta t} \phi^\pm, \\ \tilde{\alpha} = (\frac{3\alpha}{2\delta t} + 1) \frac{3}{2\delta t}. \end{cases}$$

Actually, we can solve  $\phi^{n+1}$  and  $\mu^{n+1}$  directly from (3.52) and (3.53). Once we obtain  $\phi^{n+1}$ , the  $\psi^{n+1}, U^{n+1}$  is automatically given in (3.51). Furthermore, we notice

$$(3.55) \quad (P_2(\phi), \psi) = \epsilon^2 (\nabla\phi, \nabla\psi) + \frac{1}{2} (H^\dagger \phi, H^\dagger \psi) + \frac{3\beta}{2\delta t} (\phi, \psi),$$

if  $\psi$  enjoys the same boundary condition as  $\phi$  in (3.50). Therefore, the linear operator  $P_2(\phi)$  is symmetric (self-adjoint). Moreover, for any  $\phi$  with  $\int_\Omega \phi d\mathbf{x} = 0$ , we have

$$(3.56) \quad (P_2(\phi), \phi) = \epsilon^2 \|\nabla\phi\|^2 + \frac{1}{2} \|H^\dagger \phi\|^2 \geq 0,$$

where “=” is valid if and only if  $\phi \equiv 0$ .

**Remark 3.5.** One can show the well-posedness and of the linear system (3.45)-(3.48) (or (3.52)-(3.53)) similar to Theorem 3.1. Likewise, when we rewrite (3.52)-(3.53) into a linear equation using the inverse Laplace operator, we can show the linear operator is symmetric (self-adjoint) and positive definite.

The energy stability of the scheme (3.45)-(3.48) (or (3.52)-(3.53)) is presented as follows.

**Theorem 3.3.** The scheme (3.45)-(3.48) (or (3.52)-(3.53)) is unconditionally energy stable satisfying the following discrete energy dissipation law,

$$(3.57) \quad \frac{1}{\delta t}(E_{bdf2}^{n+1} - E_{bdf2}^n) \leq -\|\nabla p^{n+1}\|^2 - \beta \left\| \frac{3\phi^{n+1} - 4\phi^n + \phi^{n-1}}{2\delta t} \right\|^2 \leq 0,$$

where

$$(3.58) \quad E_{bdf2}^{n+1} = \frac{\epsilon^2}{2} \left( \frac{\|\nabla \phi^{n+1}\|^2 + \|2\nabla \phi^{n+1} - \nabla \phi^n\|^2}{2} \right) + \frac{\|U^{n+1}\|^2 + \|2U^{n+1} - U^n\|^2}{2} \\ + \frac{\alpha}{2} \frac{\|\nabla p^{n+1}\|^2 + \|2\nabla p^{n+1} - \nabla p^n\|^2}{2} - B|\Omega|.$$

*Proof.* First, from (3.45), by taking the  $L^2$  inner product with 1 and notice  $\psi^0 = 0$ , we derive

$$(3.59) \quad \left( \frac{3\alpha}{2\delta t} + 1 \right) \int_{\Omega} \psi^{n+1} d\mathbf{x} = \frac{4\alpha}{2\delta t} \int_{\Omega} \psi^n d\mathbf{x} - \frac{\alpha}{2\delta t} \int_{\Omega} \psi^{n-1} d\mathbf{x} = 0.$$

where we use  $\int_{\Omega} \psi^1 d\mathbf{x} = 0$ , this is valid since  $\psi^1$  can be obtained using the Crank-Nicolson scheme.

Second, we combine (3.45) and (3.46) together and applying the  $\Delta^{-1}$  to obtain

$$(3.60) \quad \alpha \Delta^{-1} \left( \frac{3\psi^{n+1} - 4\psi^n + \psi^{n-1}}{2\delta t} \right) + \Delta^{-1} \psi^{n+1} \\ = -\epsilon^2 \Delta \phi^{n+1} + U^{n+1} H^\dagger + \beta \frac{3\phi^{n+1} - 4\phi^n + \phi^{n-1}}{2\delta t}.$$

Third, by taking the  $L^2$  inner product of (3.36) with  $3\phi^{n+1} - 4\phi^n + \phi^{n-1}$ , and applying the following identity

$$(3.61) \quad (3a - 4b + c, 2a) = a^2 - b^2 + (2a - b)^2 - (2b - c)^2 + (a - 2b + c)^2,$$

we obtain

$$(3.62) \quad \frac{\alpha}{2\delta t} (\Delta^{-1}(3\psi^{n+1} - 4\psi^n + \psi^{n-1}), 3\phi^{n+1} - 4\phi^n + \phi^{n-1}) + (\Delta^{-1}\psi^{n+1}, 3\phi^{n+1} - 4\phi^n + \phi^{n-1}) \\ = \frac{\epsilon^2}{2} \left( \|\nabla \phi^{n+1}\|^2 - \|\nabla \phi^n\|^2 + \|2\nabla \phi^{n+1} - \nabla \phi^n\|^2 - \|2\nabla \phi^n - \nabla \phi^{n-1}\|^2 \right. \\ \left. + \|3\nabla \phi^{n+1} - 4\nabla \phi^n - \nabla \phi^{n-1}\|^2 \right) \\ + (U^{n+1} H^\dagger, 3\phi^{n+1} - 4\phi^n + \phi^{n-1}) + \frac{\beta}{2\delta t} \|3\phi^{n+1} - 4\phi^n + \phi^{n-1}\|^2.$$

Third, by taking the  $L^2$  inner product of (3.15) with  $-2U^{n+1}$ , we obtain

$$(3.63) \quad -(\|U^{n+1}\|^2 - \|U^n\|^2 + \|2U^{n+1} - U^n\|^2 - \|2U^n - U^{n-1}\|^2 + \|U^{n+1} - 2U^n + U^{n-1}\|^2) \\ = -(H^\dagger(3\phi^{n+1} - 4\phi^n + \phi^{n-1}), U^{n+1}).$$

Fourth, define  $p^{n+1} = \Delta^{-1}\psi^{n+1}$ , by subtracting with the  $n$  and  $n-1$ -step, we obtain

$$(3.64) \quad \Delta(3p^{n+1} - 4p^n + p^{n-1}) = 3\psi^{n+1} - 4\psi^n + \psi^{n-1}.$$

From (3.48) and (3.64), we derive

$$\begin{aligned}
(3.65) \quad & \frac{\alpha}{2\delta t}(\Delta^{-1}(3\psi^{n+1} - 4\psi^n + \phi^{n-1}), 3\phi^{n+1} - 4\phi^n + \phi^{n-1}) \\
&= \alpha(3p^{n+1} - 4p^n + p^{n-1}, \psi^{n+1}) \\
&= \alpha(3p^{n+1} - 4p^n + p^{n-1}, \Delta p^{n+1}) \\
&= -\frac{\alpha}{2}(\|\nabla p^{n+1}\|^2 - \|\nabla p^n\|^2 + \|2\nabla p^{n+1} - \nabla p^n\|^2 - \|2\nabla p^n - \nabla p^{n-1}\|^2 \\
&\quad + \|\nabla p^{n+1} - 2\nabla p^n + \nabla p^{n-1}\|^2),
\end{aligned}$$

and

$$\begin{aligned}
(3.66) \quad & (\Delta^{-1}\psi^{n+1}, 3\phi^{n+1} - 4\phi^n + \phi^{n-1}) = 2\delta t(p^{n+1}, \psi^{n+1}) = 2\delta t(p^{n+1}, \Delta p^{n+1}) \\
&= -2\delta t\|\nabla p^{n+1}\|^2.
\end{aligned}$$

Finally, by combining (3.62), (3.63), (3.65) and (3.66), we obtain

$$\begin{aligned}
& \frac{\epsilon^2}{2}(\|\nabla \phi^{n+1}\|^2 - \|\nabla \phi^n\|^2 + \|2\nabla \phi^{n+1} - \nabla \phi^n\|^2 - \|2\nabla \phi^n - \nabla \phi^{n-1}\|^2 + \|\nabla \phi^{n+1} - 2\nabla \phi^n + \nabla \phi^{n-1}\|^2) \\
&+ \|U^{n+1}\|^2 - \|U^n\|^2 + \|2U^{n+1} - U^n\|^2 - \|2U^n - U^{n-1}\|^2 + \|U^{n+1} - 2U^n + U^{n-1}\|^2 \\
&+ \frac{\alpha}{2}(\|\nabla p^{n+1}\|^2 - \|\nabla p^n\|^2 + \|2\nabla p^{n+1} - \nabla p^n\|^2 - \|2\nabla p^n - \nabla p^{n-1}\|^2 + \|\nabla p^{n+1} - 2\nabla p^n + \nabla p^{n-1}\|^2) \\
&= -2\delta t\|\nabla p^{n+1}\|^2 - \frac{\beta}{2\delta t}\|3\phi^{n+1} - 4\phi^n + \phi^{n-1}\|^2.
\end{aligned}$$

That concludes the theorem.  $\square$

**Remark 3.6.** The new variable  $U$  is introduced in order to handle the nonlinear bulk potential  $F(\phi)$ . We notice that the discrete energy still includes the gradient term of  $\phi$ . Due to the Poincare inequality and mass conservation property for Cahn-Hilliard equation  $\int_{\Omega} \phi^{n+1} d\mathbf{x} = \int_{\Omega} \phi^0 d\mathbf{x}$ , the  $H^1$  stability for the variable  $\phi$  is still valid for the proposed scheme, which makes it possible to implement the rigorous error analysis for the proposed schemes. We will implement such analysis in the future work.

**Remark 3.7.** Heuristically, the  $\frac{1}{\delta t}(E_{bdf2}^{n+1} - E_{bdf2}^n)$  is a second order approximation of  $\frac{d}{dt}E(\phi, U)$  at  $t = t^{n+1}$ . For instance, for any smooth variable  $S$  with time, one can write

$$\begin{aligned}
& \left( \frac{\|S^{n+1}\|^2 + \|2S^{n+1} - S^n\|^2}{2\delta t} \right) - \left( \frac{\|S^n\|^2 + \|2S^n - S^{n-1}\|^2}{2\delta t} \right) \\
& \cong \left( \frac{\|S^{n+2}\|^2 - \|S^n\|^2}{2\delta t} \right) + O(\delta t^2) \cong \frac{d}{dt}\|S(t^{n+1})\|^2 + O(\delta t^2).
\end{aligned}$$

#### 4. NUMERICAL TESTS.

In this section, we present various numerical experiments in 2D and 3D to validate the theories derived in the previous section and demonstrate the efficiency, energy stability and accuracy of the proposed numerical schemes. In all examples, we set the domain  $\Omega = [0, 1]^d, d = 2, 3$ . We use the second order central finite difference method to discretize the space operators in the semi-discretized model. In all simulations, we set  $\epsilon = 0.01$ , and  $\alpha, \beta$  will be chosen accordingly. Since the numerical solutions using the Flory-Huggins potential are essentially the same as the double-well potential, we only present the results for the model with double-well potential.

**4.1. Convergence test.** We first test the convergence rates of the two proposed schemes, the Crank-Nicolson scheme (3.13)-(3.16) (denoted by CN2) and the BDF2 scheme (3.45)-(3.48) (denoted by BDF2). We use the following initial condition as

$$(4.1) \quad \phi = 0.5 \left( 1 + \max \left( \tanh \frac{0.2 - R_1}{\epsilon}, \tanh \frac{0.2 - R_2}{\epsilon} \right) \right),$$

where  $R_1 = \sqrt{(x - 0.71)^2 + (y - 0.5)^2}$ ,  $R_2 = \sqrt{(x - 0.29)^2 + (y - 0.5)^2}$ . The initial profile of  $\phi$  is shown in the first subfigure in Fig. 2. We use  $256 \times 256$  grid points to discretize the space so that the errors from the spatial discretization is negligibly small compared with the time discretization error. We perform the mesh refinement test in time to obtain the order of convergence in time by taking a linear refinement path for time step  $\delta t = \frac{0.01}{2^k}$ ,  $k = 0, 1, \dots, 6$ . The numerical errors are calculated as the difference between the solution of coarse time step and that of the adjacent finer time step. We plot the caughty sequence of  $L^2$  errors at  $t = 4$  with different time step sizes in Fig. 1 and the convergence rate is shown to be second order for both schemes.

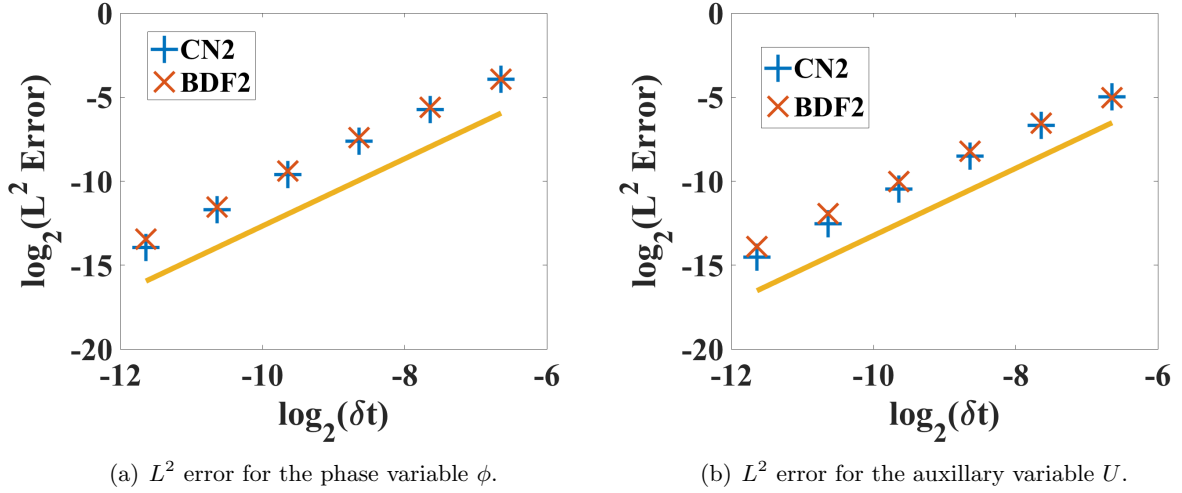


FIG. 1. Convergence test for the  $L^2$  errors for  $\phi$  and  $U$  computed by the the second order scheme CN2 and BDF2 using different temporal resolutions at  $t = 4$ . The time step is  $\delta t = 0.01(\frac{1}{2})^k$  for  $k = 0, 1, 2, 3, 4, 5, 6$  and the numerical errors are calculated as the difference between the solution of the coarse time step and that of the adjacent finner time step.

**4.2. The viscous and hyperbolic relaxation effects for the coalescence of two kissing bubbles.** In this example, we study the coalescence dynamics of two kissing bubbles by varying the viscous and hyperbolic relaxation parameters  $\alpha$  and  $\beta$ . The computational domain  $\Omega$  is still  $[0, 1]^2$  and the initial profile are the same as the one used in the previous example, and we use the CN2 scheme and  $128^2$  grid points to discretize the domain.

We start with the classical Cahn-Hilliard equation by setting  $\alpha = \beta = 0$ . In Fig. 2, due to the surface tension effect, the two bubbles coalesces into one big bubble that is in a lower free energy state. We further set the hyperbolic relaxation parameter  $\alpha = 1$  while keeping viscous parameter of  $\beta = 0$ . The numerical result in shown in Fig. 3. At  $t = 1$  and 2, the interface of the circle shows some sawtooth profile and eventually forms a circle, i.e. the Cahn-Hilliard equation with

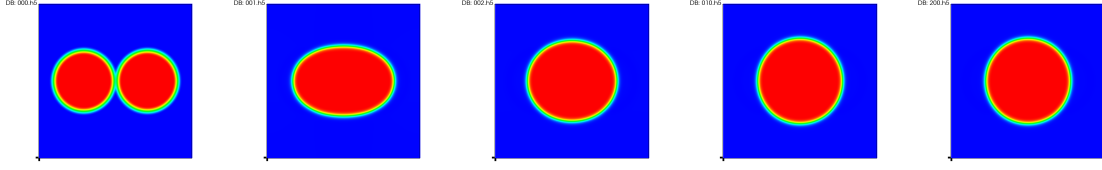


FIG. 2. Time evolution of the drop in 2D when  $\beta = 0$  and  $\alpha = 0$ . Snapshots are taken at  $t = 0, 1, 2, 10, 200$ .

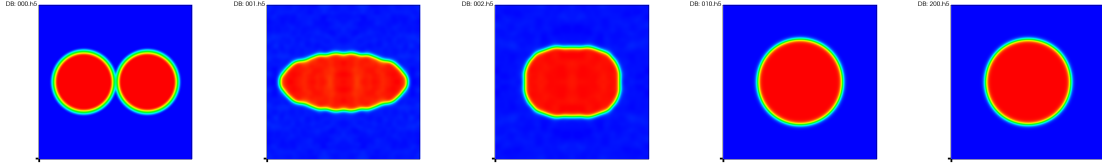


FIG. 3. Time evolution of the drop in 2D when  $\beta = 0$  and  $\alpha = 1$ . Snapshots are taken at  $t = 0, 1, 2, 10, 200$ .

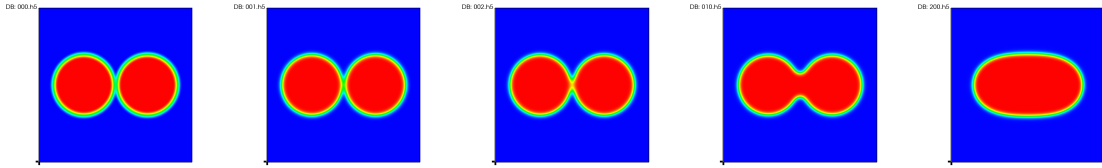


FIG. 4. Time evolution of the drop in 2D when  $\beta = 1$  and  $\alpha = 0$ . Snapshots are taken at  $t = 0, 1, 2, 10, 200$ .

hyperbolic relaxation term produces different dynamics, but the same final steady state. Afterward, we investigate the viscous effect by setting  $\beta = 1$  and  $\alpha = 0$ . The numerical results are illustrated in Fig. 4. We observe that the coalesce speed is much slower than the two previous cases where  $\beta = 0$ .

In Fig. 5, we plot the evolution of energy curves for nine cases, when both  $\alpha$  and  $\beta$  take all three values of 0, 0.5, 1. We find that  $\beta$  can dramatically affect the speed of coalesces than  $\alpha$  does, that is, the larger the viscosity is, the slower the two kissing bubbles coalesce.

**4.3. Spinodal Decomposition in 3D.** In this example, we study the phase separation dynamics in 3D that is called “spinodal decomposition”. The process of the phase separation can be studied by considering a homogeneous binary mixture, which is quenched into the unstable part of its miscibility gap. In this case, the spinodal decomposition takes place, which manifests in the spontaneous growth of the concentration fluctuations that leads the system from the homogeneous to the two-phase state. Shortly after the phase separation starts, the domains of the binary components are formed and the interface between the two phases can be specified [1, 13, 68].

The initial conditions are taken as the randomly perturbed concentration fields as follows,

$$(4.2) \quad \phi_0(x, y, z) = \bar{\phi}_0 + 0.001\text{rand}(x, y, z),$$

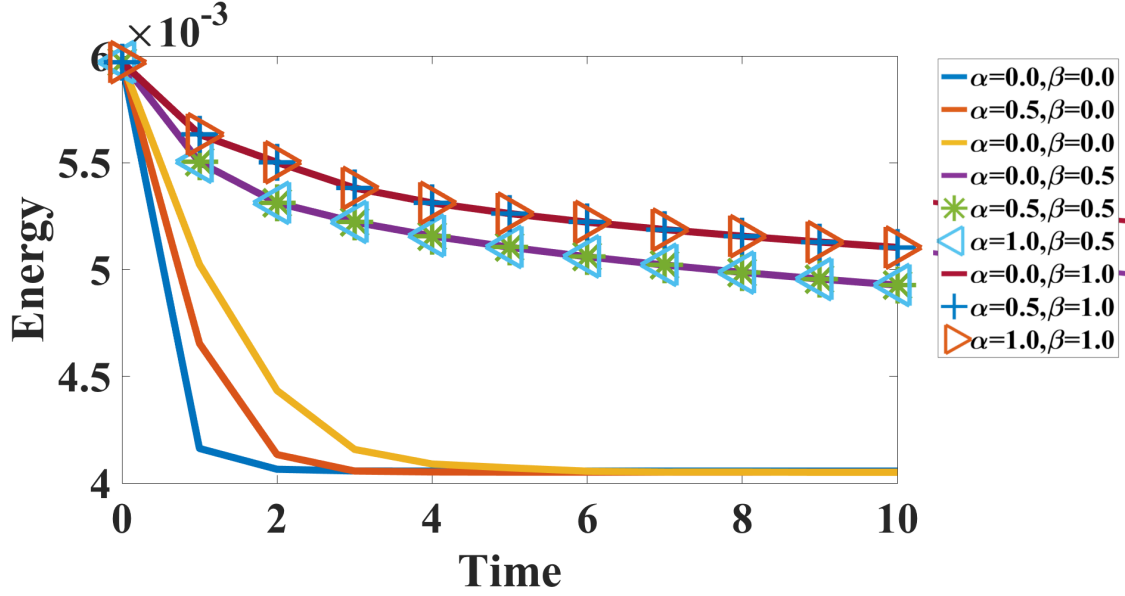


FIG. 5. Time evolution of the free energy functional for the coalescence of two kissing bubbles for nine choices of order parameters  $\alpha = 0, 0.5, 1$ , and  $\beta = 0, 0.5, 1$ .

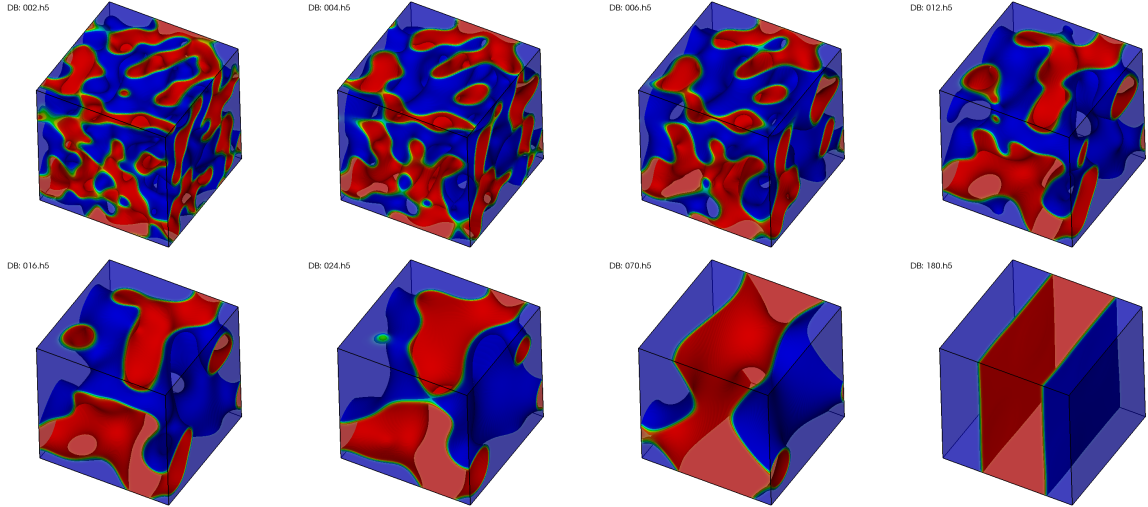


FIG. 6. 3D spinodal decomposition for random initial data with  $\bar{\phi}_0 = 0.5$ . Snapshots of the phase variables  $\phi$  are taken at  $t = 20, 40, 60, 120, 160, 240, 700$ , and  $1800$ . The order parameters are  $\alpha = 0$  and  $\beta = 0.9$ .

where the  $\text{rand}(x, y, z)$  represents the random number in  $[-1, 1]$  and has zero mean. The computational domain is  $[0, 2\pi]^3$  and we use the scheme CN2 and  $128^3$  grid points to discretize the domain, the time step is  $\delta t = 0.001$  for all 3D simulations.

From the 2D tests, we know the viscous parameter  $\beta$  can have more effects on the dynamics than the hyperbolic parameter  $\alpha$ . Thus in the following 3D simulations, we simply set  $\beta = 0.9$  and  $\alpha = 0$ .

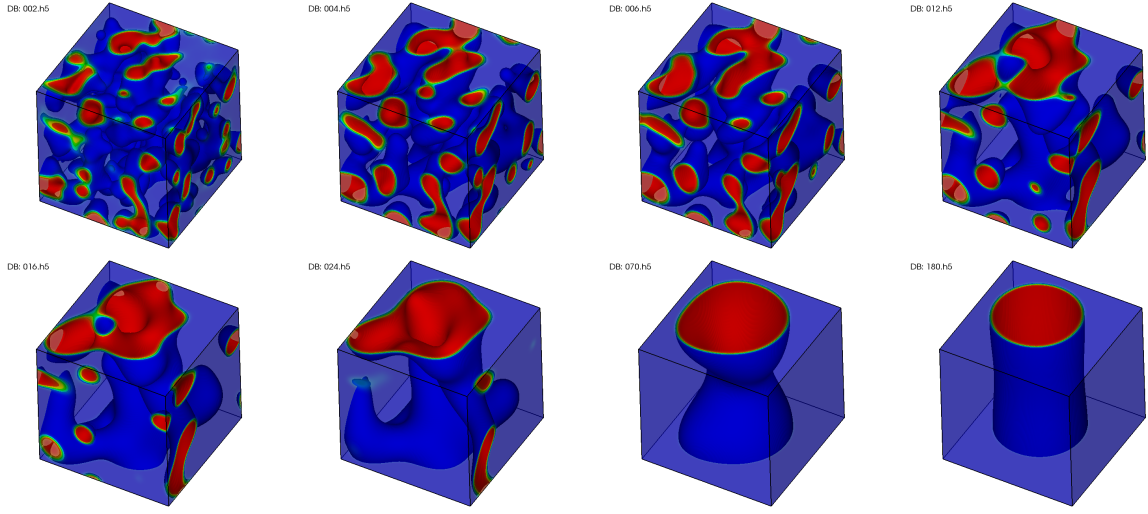


FIG. 7. 3D spinodal decomposition for random initial data with  $\bar{\phi}_0 = 0.3$ . Snapshots of the phase variables  $\phi$  are taken at  $t = 20, 40, 60, 120, 160, 240, 700$  and  $2000$ . The order parameters are  $\alpha = 0$  and  $\beta = 0.9$ .

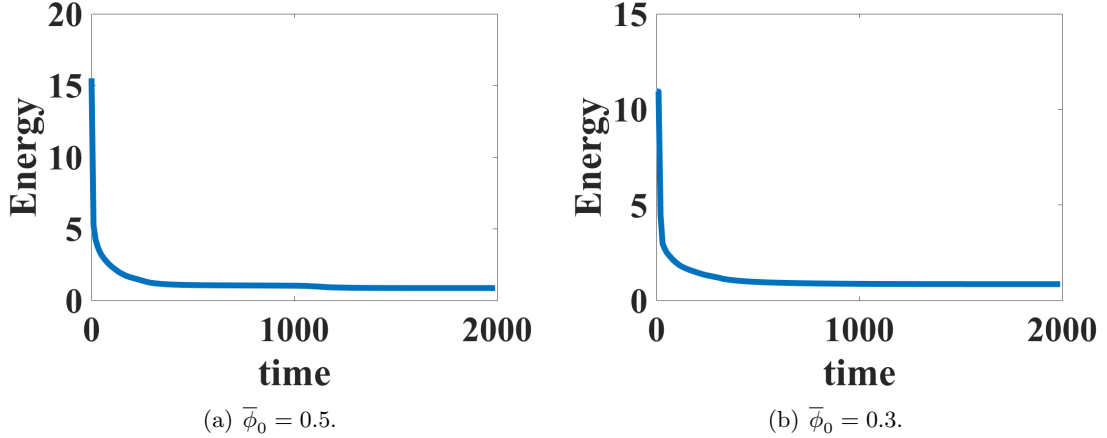


FIG. 8. Time evolution of the free energy functional for spinodal decomposition for the cases of  $\bar{\phi}_0 = 0.5$  and  $\bar{\phi}_0 = 0.3$ , respectively. The order parameters are  $\alpha = 0, \beta = 0.9$ .

The red domain, corresponding to the larger values of  $\phi = 1$ , indicates the concentrated polymer segments [22], and the blue region, corresponding to the smaller values of  $\phi = -1$ , indicates the macromolecular microspheres (MMS). In Fig. 6, we perform numerical simulations for the initial profile  $\bar{\phi}_0 = 0.5$ , that means the volume fraction of the polymer segments are almost same as the surrounding MMS. The final steady state forms the uniform two layer structure around  $t = 1800$ . Fig. 7 shows the dynamical behaviors of the phase separation for the initial value  $\bar{\phi}_0 = 0.3$  which means the volume of the MMS are much more than that of the polymer segments. We observe that the MMS finally accumulate together to the cylindrical shape. In Fig. 8, we plot the evolution of



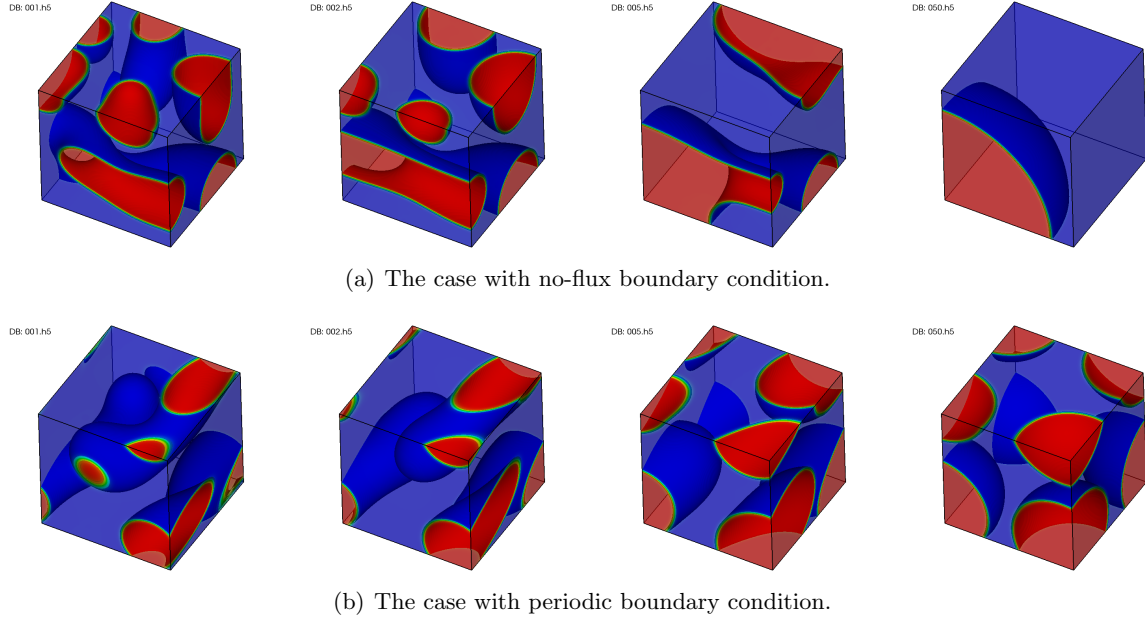


FIG. 9. 3D spinodal decomposition for random initial data with  $\bar{\phi}_0 = 0.3$  for no-flux and periodic boundary conditions. Snapshots are taken at  $t = 1, 2, 5, 50$ . The order parameters are  $\alpha = \beta = 0$  for both cases.

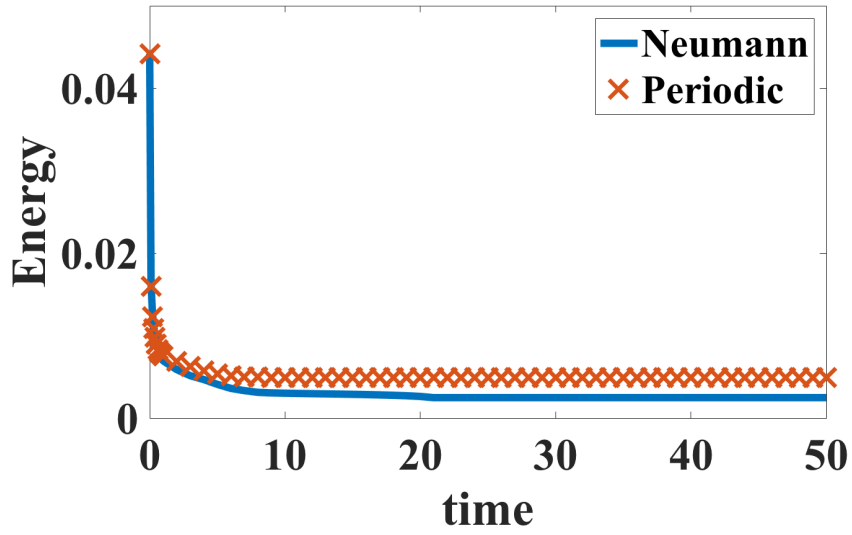


FIG. 10. Time evolution of the free energy functional for spinodal decomposition for no-flux and periodic boundary conditions with  $\bar{\phi}_0 = 0.3, \alpha = \beta = 0$ .

energy curves for both cases, where we observe that the total free energy decreases to the steady state monotonically.

Note the boundary conditions of the governing system can be the periodic or no-flux, in Fig. 9, we perform numerical simulations for the initial profile of  $\bar{\phi}_0 = 0.3$  and  $\alpha = \beta = 0$  for these two boundary conditions. For both cases, we observe that the MMS finally accumulate together to the spherical shape, where the final shape is  $1/8$  spherical segment at a corner for no-flux condition, and a sphere for the period boundary condition (with parts at each corner of the cube). We plot the evolution of energy curves for both cases in Fig. 10. And we observe the energy of the spherical segment with no-flux boundary condition is smaller than that of the sphere in the period boundary condition.

## 5. CONCLUDING REMARKS

In this paper, we develop two second-order in time schemes to solve the VCH-HR system by utilizing the novel IEQ approach. The developed schemes (i) are *accurate* (second order in time); (ii) are *stable* (unconditional energy dissipation law holds); and (iii) are *easy to implement* (only need to solve linear equations at each time step). Furthermore, the induced linear system is symmetric positive definite, thus one can apply any Krylov subspace methods with mass lumping as pre-conditioners for solving such system efficiently. Although we consider only time discrete schemes in this study, the results can be carried over to any consistent finite-dimensional Galerkin approximations since the proofs are all based on a variational formulation with all test functions in the same space as the space of the trial functions.

**Acknowledgments.** X. Yang is partially supported by NSF DMS-1200487 and NSF DMS-1418898.

## REFERENCES

- [1] K. Binder. Collective diffusion, nucleation, and spinodal decomposition in polymer mixtures. *J. Chem. Phys.*, 79:6387, 1983.
- [2] E. Bonetti, W. Dreyer, and G. Schimperna. Global Solutions to a Viscous Cahn-Hilliard Equation for Tin-lead Alloys with Mechanical Stresses. *Adv. Diff. Eqn.*, pages 231–256, 2003.
- [3] A. Bonfoh, M. Grasselli, and A. Miranville. Singularly perturbed 1D Cahn–Hilliard equation revisited. *Nonlinear Differ. Equ. Appl.*, pages 663–695, 2010.
- [4] F. Boyer and S. Minjeaud. Numerical schemes for a three component cahn-hilliard model. *ESAIM: M2AN*, 45:697–738, 2011.
- [5] J. W. Cahn and J. E. Hilliard. Free energy of a nonuniform system. I. interfacial free energy. *J. Chem. Phys.*, 28:258–267, 1958.
- [6] A. N. Carvalho and T. Dlotko. Dynamics of the viscous Cahn–Hilliard equation. *J. Math. Anal. Appl.*, 344:703–725, 2008.
- [7] L. Q. Chen and Y. Wang. The continuum field approach to modeling microstructural evolution. *JOM*, 48:13–18, 1996.
- [8] R. Chen, G. Ji, X. Yang, and H. Zhang. Decoupled energy stable schemes for phase-field vesicle membrane model. *J. Comput. Phys.*, 302:509–523, 2015.
- [9] S. M. Choo and S. K. Chung. Asymptotic behaviour of the viscous cahn-hilliard equation. *Journal of Applied Mathematics and Computing*, 11(1):143–154, 2003.
- [10] P. Colli, G. Gilardi, and J. Sprekels. A boundary control problem for the viscous cahn—hilliard equation with dynamic boundary conditions. *Appl. Math. Optim.*, 73(2):195–225, 2016.
- [11] M. Conti and G. Mola. 3D viscous Cahn–Hilliard equation with memory. *Math. Meth. Appl. Sci.*, pages 1370–1395, 2009.
- [12] M. I. M. Copetti and C. M. Elliott. Numerical analysis of the cahn-hilliard equation with a logarithmic free energy. *Numer. Math.*, 63(4):39–65, 1992.

- [13] P. G. de Gennes. Dynamics of fluctuations and spinodal decomposition in polymer blends. *J. Chem. Phys.*, 7:4756, 1980.
- [14] T. Dlotko and C. Sun. Dynamics of the modified viscous cahn-hilliard equation in  $\mathbb{R}^n$ . *Topol. Methods. Nonlinear. Anal.*, 35(2):277–294., 2010.
- [15] W. Dreyer and C. Gohlke. Sharp limit of the viscous cahn–hilliard equation and thermodynamic consistency. *Cont. Mech. Thermo.*, pages 1–22, 2015.
- [16] Q. Du, C. Liu, and X. Wang. Phase field approach in the numerical study of the elastic bending energy for vesicle membranes. *J. Comput. Phys.*, 198:450–468, 2004.
- [17] C. Dupaix, D. Hilhorst, and I. N .Kostin. The viscous Cahn–Hilliard equation as a limit of the phase field model: lower semi continuity of the attractor. *J. Dyn. Diff. Eqns.*, 11:333–353, 1999.
- [18] C. M. Elliott. Viscous Cahn-Hilliard equation II. Analysis. *J. Diff. Eqn.*, 128:387–414, 1996.
- [19] C. M. Elliott and I. K. Kostin. Lower semicontinuity of a non-hyperbolic attractor for the viscous Cahn–Hilliard equation. *Nonlinearity*, 9:687–702, 1996.
- [20] D. J. Eyre. Unconditionally gradient stable time marching the Cahn-Hilliard equation. In *Computational and mathematical models of microstructural evolution (San Francisco, CA, 1998)*, volume 529 of *Mater. Res. Soc. Sympos. Proc.*, pages 39–46. MRS, 1998.
- [21] X. Feng and A. Prol. Numerical analysis of the allen-cahn equation and approximation for mean curvature flows. *Numer. Math.*, 94:33–65, 2003.
- [22] M. Fialkowski and R. Holyst. Dynamics of phase separation in polymer blends revisited: morphology, spinodal, noise, and nucleation. *Macromol. Theory Simul.*, 17:263, 2008.
- [23] P. Galenko. Phase-field models with relaxation of the diffusion flux in nonequilibrium solidification of a binary system. *Phys. Lett. A*, pages 190–197, 2001.
- [24] P. Galenko and D. Jou. Diffuse-interface model for rapid phase transformations in nonequilibrium systems. *Phys. Rev. E*, page 046125, 2005.
- [25] P. Galenko and D. Jou. AKinetic contribution to the fast spinodal decomposition controlled by diffusion. *Phys. A*, pages 3113–3123, 2009.
- [26] P. Galenko and V. Lebedev. Analysis of the dispersion relation in spinodal decomposition of a binary system. *Philos. Mag. Lett.*, pages 821–837, 2007.
- [27] P. Galenko and V. Lebedev. Local nonequilibrium effect on spinodal decomposition in a binary system. *Int. J. Thermodyn.*, pages 21–28, 2008.
- [28] P. Galenko and V. Lebedev. Nonequilibrium effects in spinodal decomposition of a binary system. *Phys. Lett. A*, pages 985–989, 2008.
- [29] S. Gatti, M. Grasselli, V. Pata, and A. Miranville. Hyperbolic relaxation of the viscous Cahn–Hilliard equation in 3-D. *Math. Models and Meth. in Appl. Sci.*, 15(02):165–198, 2005.
- [30] M. Grinfeld and A. Novick-Cohen. The viscous Cahn-Hilliard equation: morse decomposition and structure of the global attractor. *Trans. Amer. Math. Soc.*, 351(6):2375–2406, 1999.
- [31] Z. Guan, J. S.Lowengrub, C. Wang, and S. M. Wise. Second order convex splitting schemes for periodic nonlocal cahn–hilliard and allen–cahn equations. *J. Comput. Phys.*, 277:48–71, 2014.
- [32] F. Guillén-González and G. Tierra. On linear schemes for a Cahn-Hilliard diffuse interface model. *J. Comput. Phys.*, 234:140–171, 2013.
- [33] M. B. Kania. Upper semicontinuity of global attractors for the perturbed viscous Cahn-Hilliard equations. *Topol. Methods Nonlinear Anal.*, pages 327–345, 2008.
- [34] J. Kim. Phase-field models for multi-component fluid flows. *Comm. Comput. Phys*, 12(3):613–661, 2012.
- [35] N. Lecoq, H. Zapolsky, and P. Galenko. Evolution of the structure factor in a hyperbolic model of spinodal decomposition. *Eur. Phys. J. Spec. Topics*, pages 165–175, 2009.
- [36] C. Liu and J. Shen. A phase field model for the mixture of two incompressible fluids and its approximation by a Fourier-spectral method. *Physica D*, 179(3-4):211–228, 2003.
- [37] C. Liu, J. Shen, and X. Yang. Dynamics of defect motion in nematic liquid crystal flow: Modeling and numerical simulation. *Comm. Comput. Phys.*, 2:1184–1198, 2007.
- [38] C. Liu, J. Shen, and X. Yang. Decoupled energy stable schemes for a phase filed model of two-phase incompressible flows with variable density. *J. Sci. Comput.*, 62:601–622, 2015.
- [39] J. S. Lowengrub, A. Ratz, and A. Voigt. Phase field modeling of the dynamics of multicomponent vesicles spinodal decomposition coarsening budding and fission. *Phys. Rev. E*, 79(3), 2009.
- [40] P. O. Mchedlov-petrosyan. The convective viscous Cahn-Hilliard equation: Exact solutions. *Euro. J. of Appl. Math.*, 27(1):42–65, 2016.

- [41] C. Miehe, M. Hofacker, and F. Welschinger. A phase field model for rate-independent crack propagation: Robust algorithmic implementation based on operator splits. *Comput. Meth. in Appl. Mech. and Engrg.*, 199:2765–2778, 2010.
- [42] R. H. Nochetto, A. J. Salgado, and I. Tomas. A diffuse interface model for two-phase ferrofluid flows. *Comput. Meth. in Appl. Mech. and Engrg.*, 309:497–531, 2016.
- [43] A. Novick-Cohen. On the viscous Cahn–Hilliard equation. in *Material Instabilities in Continuum Mechanics (Edinburgh, 1985–1986)*, ed. J. M. Ball (Oxford University Press), 128:329–342, 1988.
- [44] R. Rossi. On two classes of generalized viscous Cahn-Hilliard equations. *Comm. Pure. Appl. Anal.*, pages 405–430, 2005.
- [45] R. Scala and G. Schimperna. On the viscous cahn-hilliard equation with singular potential and inertial term, 2016.
- [46] J. Shen, T. Tang, and J. Yang. On the maximum principle preserving schemes for the generalized Allen-Cahn Equation. *Comm. Math. Sci.*, 14:1517–1534, 2016.
- [47] J. Shen and X. Yang. An efficient moving mesh spectral method for the phase-field model of two-phase flows. *J. Comput. Phys.*, 228:2978–2992, 2009.
- [48] J. Shen and X. Yang. Energy stable schemes for Cahn-Hilliard phase-field model of two-phase incompressible flows. *Chinese Ann. Math. series B*, 31:743–758, 2010.
- [49] J. Shen and X. Yang. Numerical approximations of Allen-Cahn and Cahn-Hilliard equations. *Disc. Conti. Dyn. Sys.-A*, 28:1669–1691, 2010.
- [50] J. Shen and X. Yang. A phase field model and its numerical approximation for two phase incompressible flows with different densities and viscosities. *SIAM J. Sci. Comput.*, 32:1159–1179, 2010.
- [51] J. Shen and X. Yang. Decoupled energy stable schemes for phase field models of two phase complex fluids. *SIAM J. of Sci. Comput.*, 36(1):122–145, 2014.
- [52] J. Shen and X. Yang. Decoupled, energy stable schemes for phase field models of two phase incompressible flows. *SIAM J. Num. Ana.*, 53:279–296, 2015.
- [53] J. Shen, X. Yang, and H. Yu. Energy stable scheme and simulation for multiphase fluids system of naiver boundary condition. *J. Comput. Phys.*, 284:617–630, 2015.
- [54] J. Shin, Y. Choi, and J. Kim. An unconditionally stable numerical method for the viscous Cahn-Hilliard equation. *Disc. Cont. Dyn. Sys. B*, 19:1734–1747, 2014.
- [55] R. Spatschek, E. Brener, and A. Karma. A phase field model for rate-independent crack propagation: Robust algorithmic implementation based on operator splits. *Philosophical Magazine*, 91:75–95, 2010.
- [56] C. Wang and S. M. Wise. An energy stable and convergent finite-difference scheme for the modified phase field crystal equation. *SIAM J. Numer. Anal.*, 49:945–969, 2011.
- [57] X. Yang. Linear, first and second-order, unconditionally energy stable numerical schemes for the phase field model of homopolymer blends. *J. Comput. Phys.*, 327:294–316, 2016.
- [58] X. Yang, J. J. Feng, C. Liu, and J. Shen. Numerical simulations of jet pinching-off and drop formation using an energetic variational phase-field method. *J. Comput. Phys.*, 218:417–428, 2006.
- [59] X. Yang, M. G. Forest, H. Li, C. Liu, J. Shen, Q. Wang, and F. Chen. Modeling and simulations of drop pinch-off from liquid crystal filaments and the leaky liquid crystal faucet immersed in viscous fluids. *J. Comput. Phys.*, 236:1–14, 2013.
- [60] X. Yang and L. Ju. Efficient linear schemes with unconditionally energy stability for the phase field elastic bending energy model. *Comput. Meth. Appl. Mech. Engrg.*, 315:691–712, 2017.
- [61] J. Zhao, H. Li, Q. Wang, and X. Yang. A linearly decoupled energy stable scheme for phase-field models of three-phase incompressible flows. *in press*, DOI: 10.1007/s10915-016-0283-9, *J. Sci. Comput.*, 2017.
- [62] J. Zhao, Q. Wang, and X. Yang. Numerical approximations for a phase field dendritic crystal growth model based on the invariant energy quadratization approach. *in press*, DOI: 10.1002/nme.5372, *Inter. J. Num. Meth. Engrg.*, 2016.
- [63] J. Zhao, Q. Wang, and X. Yang. Numerical approximations to a new phase field model for immiscible mixtures of nematic liquid crystals and viscous fluids. *Comput. Meth. Appl. Mech. Eng.*, 310:77–97, 2016.
- [64] J. Zhao, X. Yang, Y. Gong, and Q. Wang. A novel linear second order unconditionally energy stable scheme for a hydrodynamic q-tensor model of liquid crystals. *in press*, *Computer Methods in Applied Mechanics and Engineering*, 2017.
- [65] J. Zhao, X. Yang, J. Li, and Q. Wang. Energy stable numerical schemes for a hydrodynamic model of nematic liquid crystals. *SIAM. J. Sci. Comput.*, 38:A3264–A3290, 2016.

- [66] J. Zhao, X. Yang, J. Shen, and Q. Wang. A decoupled energy stable scheme for a hydrodynamic phase-field model of mixtures of nematic liquid crystals and viscous fluids. *J. Comput. Phys.*, 305:539–556, 2016.
- [67] S. Zheng and A. Milani. Global attractors for singular perturbations of the Cahn–Hilliard equations. *J. Diff. Eqn.*, 209:101–139, 2005.
- [68] J. Zhu, L. Chen, J. Shen, and V. Tikare. Coarsening kinetics from a variable-mobility cahn-hilliard equation: Application of a semi-implicit fourier spectral method. *Phys. Rev. E.*, 60(4):3564–3572, 1999.